Neuroscience 177 (2011) 240–251

ALTERED PROFILE AND D2-DOPAMINE RECEPTOR MODULATION OF HIGH VOLTAGE-ACTIVATED CALCIUM CURRENT IN STRIATAL MEDIUM SPINY NEURONS FROM ANIMAL MODELS OF PARKINSON'S DISEASE

G. MARTELLA,[a] G. MADEO,[a] T. SCHIRINZI,[a] A. TASSONE,[b] G. SCIAMANNA,[b] F. SPADONI,[a] A. STEFANI,[a] J. SHEN,[c] A. PISANI[a,b]* AND P. BONSI[b]

[a]*Department of Neuroscience, University Tor Vergata, Via Montpellier 1, 00133 Rome, Italy*

[b]*Laboratory of Neurophysiology and Plasticity, Fondazione Santa Lucia I.R.C.C.S., Via del Fosso di Fiorano 64, 00143 Rome, Italy*

[c]*Center for Neurologic Diseases, Brigham and Women's Hospital, Program in Neuroscience, Harvard Medical School, 77 Avenue Louis Pasteur, Boston, MA 02115-5727, USA*

Abstract—In the present work we analyzed the profile of high voltage-activated (HVA) calcium (Ca^{2+}) currents in freshly isolated striatal medium spiny neurons (MSNs) from rodent models of both idiopathic and familial forms of Parkinson's disease (PD). MSNs were recorded from reserpine-treated and 6-hydroxydopamine (6-OHDA)-lesioned rats, and from DJ-1 and PINK1 (PTEN induced kinase 1) knockout ($^{-/-}$) mice. Our analysis showed no significant changes in total HVA Ca^{2+} current. However, we recorded a net increase in the L-type fraction of HVA Ca^{2+} current in dopamine-depleted rats, and of both N- and P-type components in DJ-$1^{-/-}$ mice, whereas no significant change in Ca^{2+} current profile was observed in PINK$1^{-/-}$ mice. Dopamine modulates HVA Ca^{2+} channels in MSNs, thus we also analyzed the effect of D1 and D2 receptor activation. The effect of the D1 receptor agonist SKF 83822 on Ca^{2+} current was not significantly different among MSNs from control animals or PD models. However, in both dopamine-depleted rats and DJ-$1^{-/-}$ mice the D2 receptor agonist quinpirole inhibited a greater fraction of HVA Ca^{2+} current than in the respective controls. Conversely, in MSNs from PINK$1^{-/-}$ mice we did not observe alterations in the effect of D2 receptor activation. Additionally, in both reserpine-treated and 6-OHDA-lesioned rats, the effect of quinpirole was occluded by the selective L-type Ca^{2+} channel blocker nifedipine, while in DJ-$1^{-/-}$ mice it was mostly occluded by ω-conotoxin GVIA, blocker of N-type channels. These results demonstrate that both dopamine depletion and DJ-1 deletion induce a rearrangement in the HVA Ca^{2+} channel profile, specifically involving those channels that are selectively modulated by D2 receptors. © 2011 IBRO. Published by Elsevier Ltd. All rights reserved.

Key words: HVA calcium channels, medium spiny neuron, 6-hydroxydopamine, reserpine, DJ-1, PINK1.

*Correspondence to: A. Pisani, Dipartimento di Neuroscienze, Università Tor Vergata, Via Montpellier 1, 00133 Rome, Italy. Tel: +39-06-72596010; fax: +39-06-72596006.
E-mail address: pisani@uniroma2.it (A. Pisani).

Abbreviations: CN, cell capacitance; HBSS, Hank's balanced salt solution; HVA, high voltage-activated; MSNs, medium spiny neurons; PD, Parkinson's disease; PINK1, PTEN induced kinase 1; SNpc, substantia nigra pars compacta; 6-OHDA, 6-hydroxydopamine.

Parkinson's disease (PD) is a neurodegenerative movement disorder characterized by bradykinesia, rigidity, resting tremor, and postural instability. Although the occurrence of PD is largely sporadic, an increasing number of monogenic mutations in distinct genes—such as the large exonic deletions or frame-shift truncations, suggestive of a "loss of function" mechanism, found in DJ-1 and PINK1 (PTEN induced kinase 1) genes (Bonifati et al., 2003; Valente et al., 2004; Kitada et al., 2007)—has been linked to familial forms of parkinsonism, which clinically resemble idiopathic PD. The clinical features of idiopathic and familial PD are thought to result from a reduced dopaminergic input to the striatum, inducing a complex rearrangement in the functional anatomy of the basal ganglia. In particular, dopamine depletion has been shown to cause the loss of spines in medium spiny neurons (MSNs) from both animal models of PD and parkinsonian patients (for review see: Deutch et al., 2007; Smith and Villalba, 2008). This morphological alteration of MSNs has been recently ascribed to the disinhibition of Cav1.3-containing L-type Ca^{2+} channels, as a consequence of the reduced striatal dopaminergic tone (Day et al., 2006). In fact, chronic administration of an L-type channel antagonist completely prevented the spine loss induced in rats by acute DA depletion. Conversely, spine density was found to be significantly increased in *Cacna1d*$^{-/-}$ mice, lacking the Cav1.3α1 subunits. L-type Ca^{2+} channels have already been implicated in the selective degeneration of dopaminergic neurons in PD (Chan et al., 2009); these experimental data suggest that high voltage-activated (HVA) Ca^{2+} channels might play a direct role in striatal dysfunction, as well.

EXPERIMENTAL PROCEDURES

All experiments were performed in accordance with both the EC and Italian guidelines (86/609/EEC; D.Lvo 116/1992, respectively) and approved by the University of Rome "Tor Vergata" (n. 153/2001A).

Animal models

6-hydroxydopamine (6-OHDA)-lesioned rats. Dopamine denervation was obtained by injecting the neurotoxin 6-OHDA (1 mg/kg) into the substantia nigra pars compacta (SNpc) of adult male Wistar rats (150–170 g). Animals were anaesthetized with xylazine (7.5 mg/kg, i.m.) and ketamine (50 mg/kg, i.m.) and secured in a stereotaxic apparatus (Stoelting, Woodale, IL, USA). The injection of 6-OHDA into the mesencephalon was performed according to the following coordinates (from bregma): AP, −4.4; L, +1.2; DV, −7.8. After 15 days, dopamine denervation was as-

0306-4522/11 $ - see front matter
doi:10.1016/j.neuroscience.2010.12.057

sessed by apomorphine-driven test (1 mg/ml/kg). Animals showing ≥400 rotations/h ($n=17$) were used for the electrophysiological experiments. Fifteen rats were injected with saline solution in the same surgical sessions (sham-operated group).

Reserpine model. Adult Wistar rats (135–170 g) were injected i.p. with reserpine (3–4 mg/kg in 0.5% glacial acetic acid in PBS). Either 20–24 h ($n=13$) or 48 h ($n=4$) after reserpine injection rats displaying typical parkinsonian-like symptoms (bradykinesia, posture stiffness, and tremor) were used for electrophysiological recordings. Vehicle-treated controls were prepared in the same sessions ($n=15$).

Preparation of acutely dissociated striatal neurons

Coronal corticostriatal slices (450 μm thick) were cut as previously described (Martella et al., 2008) from brain tissue blocks of either male Wistar rat (125–150 g) or wild-type, DJ-1$^{-/-}$, and PINK1$^{-/-}$ mice (aged 40–45 days) generated in J. Shen laboratories (Goldberg et al., 2005; Kitada et al., 2007). Data obtained from each animal group were compared to the respective controls. Vehicle-treated and sham-operated rats were utilized as controls for the reserpinized and 6-OHDA-lesioned animals, respectively, while wild-type littermates of the same mixed genetic background were utilized as controls for either DJ-1$^{-/-}$ or PINK1$^{-/-}$ mice. In brief, animals were killed under ether anaesthesia by cervical dislocation, the brains were rapidly removed, and coronal corticostriatal slices were cut with a vibratome in ice-cold Krebs' solution (in mM: 126 NaCl, 2.5 KCl, 1.3 $MgCl_2$, 1.2 NaH_2PO_4, 2.4 $CaCl_2$, 10 glucose, and 18 $NaHCO_3$). Afterward, as previously described (Martella et al., 2008) the striatum was dissected from slices and incubated first in HEPES-buffered Hank's balanced salt solution (HBSS), bubbled with 100% O_2 at 35 °C, and then in HBSS containing 0.5 mg/ml protease XIV for 30 min. After repeated wash-out in HBSS, the tissue was mechanically triturated with a graded series of fire-polished Pasteur pipettes. The cell suspension was placed in a Petri dish mounted on the stage of an inverted microscope (Nikon Diaphot, Japan). Healthy cells were allowed to settle for about 10–15 min.

Patch-clamp recordings

Freshly isolated MSNs were identified by their morphologic and electrophysiological properties (Martella et al., 2008). Patch-clamp recordings in the whole-cell configuration were performed by using glass pipettes (WPI PG52165-4, Germany) pulled with a Flaming-Brown puller (Sutter Instrument, Novato, CA, USA) and fire-polished before use. Pipette resistance ranged from 3 to 8 MΩ. The composition of the internal solution was (in mM): N-methyl-D-glucamine, 185; HEPES, 40; EGTA, 11; $MgCl_2$, 4; phosphocreatine, 20; ATP, 2 to 3; guanosine triphosphate (GTP), 0 to 0.2; leupeptin, 0.2; pH 7.36, 280 mOsm/L. After obtaining the cell access, cells were bathed in (mM): TEA-Cl, 155; $CsCl_2$, 5; HEPES, 10; and $BaCl_2$, 5, as the charge carrier; pH 7.35, 300 mOsm/L. Control and drug solutions were applied with a linear array of six gravity-fed capillaries positioned 500–600 μm close to the patched neuron. Recordings were made with an Axopatch 1D (Axon Instrument). Electrode resistances in bath were ~3–6 MΩ. After formation of a GΩ seal and subsequent cell rupture, series resistance was compensated (75–85%) and periodically monitored. Data were low-pass filtered (corner frequency, 5 kHz). For data acquisition and analysis, pClamp 9.2 software (Axon Instruments) was used.

Total HVA Ca^{2+} current was examined by utilizing either ramp test (from −70 mV to +40 mV) or test pulse protocols (a single step from −60 mV to +10 mV; or incremental 10 mV steps from −70 to +40 mV, Fig. 1A). In order to pharmacologically identify the distinct components of HVA Ca^{2+} current, selective Ca^{2+} channel blockers were applied sequentially: L-type channel blocker nifedipine (NIFE, 1–5 μM), N-type channel blocker ω-Conotoxin GVIA (Ctx-GVIA, 1 μM), P-type channels blocker ω-agatoxin IVA (Atx-IVA, 20 nM), and Q-type channel blocker ω-Conotoxin MVIIC (Ctx-MVIIC, 100 nM). The voltage dependence of activation was determined from measurements of tail current amplitude, which was expected to reflect the fraction of Ca^{2+} channels opened during the preceding depolarization.

Data analysis

Voltage-activated currents were leak subtracted. Cells exhibiting leak currents >10 pA were not included in this analysis. Cell capacitance (C_m) was monitored using the automated function of the Axopatch amplifier. A stable C_m-value over time was an important criterion for the evaluation of the quality of experiments. Statistical tests were performed using Microcal Origin (OriginLab, Northampton, MA, USA) and GraphPad Prism (GraphPad Software, San Diego, CA, USA) softwares. Values given in the text and in the figures are mean±SD of changes in the respective cell populations, unless otherwise stated. The *t*-test or Mann–Whitney test were used for assessing statistical significance where appropriate. Multiple groups were compared using one-way or two-way ANOVA. The Tukey HSD test was used for post hoc comparison of the ANOVA. Values were considered statistically significant when $P<0.05$ with $\alpha=0.001$.

Drug source

Nifedipine, ω-conotoxin GVIA, and ω-agatoxin IVA were from Tocris-Cookson, UK. All other compounds used were purchased from Sigma-Aldrich, Italy.

RESULTS

Increased L-type Ca^{2+} current fraction in striatal MSNs from dopamine-depleted rats

Two different experimental approaches were utilized to obtain striatal dopamine depletion modelling idiopathic PD (for review see: Bonsi et al., 2006; Gubellini et al., 2010). In a group of male Wistar rats ($n=17$) the neurotoxin 6-OHDA (1 mg/kg; Baunez et al., 1995) was delivered into the SNpc by sterotactic injection. In the same surgical sessions, saline was injected into the SNpc of another group of 15 rats (sham-operated group). Furthermore, in a different group of animals endogenous amines were depleted by 3–4 mg/kg, i.p. reserpine treatment (Harrison et al., 2001) and after 24 ($n=13$) or 48 h ($n=4$) rats manifesting typical parkinsonian-like symptoms were utilized for the experiments (Baunez et al., 1995; Spadoni et al., 2004). Vehicle-treated controls were prepared in the same sessions ($n=15$).

Total HVA Ca^{2+} current was recorded from 173 MSNs acutely isolated from the striata of either vehicle- and reserpine-treated rats, or 6-OHDA-lesioned and sham-operated rats (Fig. 1A). Peak amplitude of the current was not statistically different either between vehicle- (625.7±23.6 pA; $n=43$), and reserpine-treated rats (627.6±33.2 pA; $n=45$; $P>0.05$ Mann–Whitney test; not shown), or between sham-operated (671.8±35.4 pA; $n=41$) and 6-OHDA-lesioned rats (611.2±21.2 pA; $n=44$; $P>0.05$ Mann–Whitney test; not shown). Moreover, the amplitude of total HVA Ca^{2+} current was not statistically different between the groups ($P>0.05$ ANOVA followed by Tukey HSD test). In order to rule out changes in cell surface area

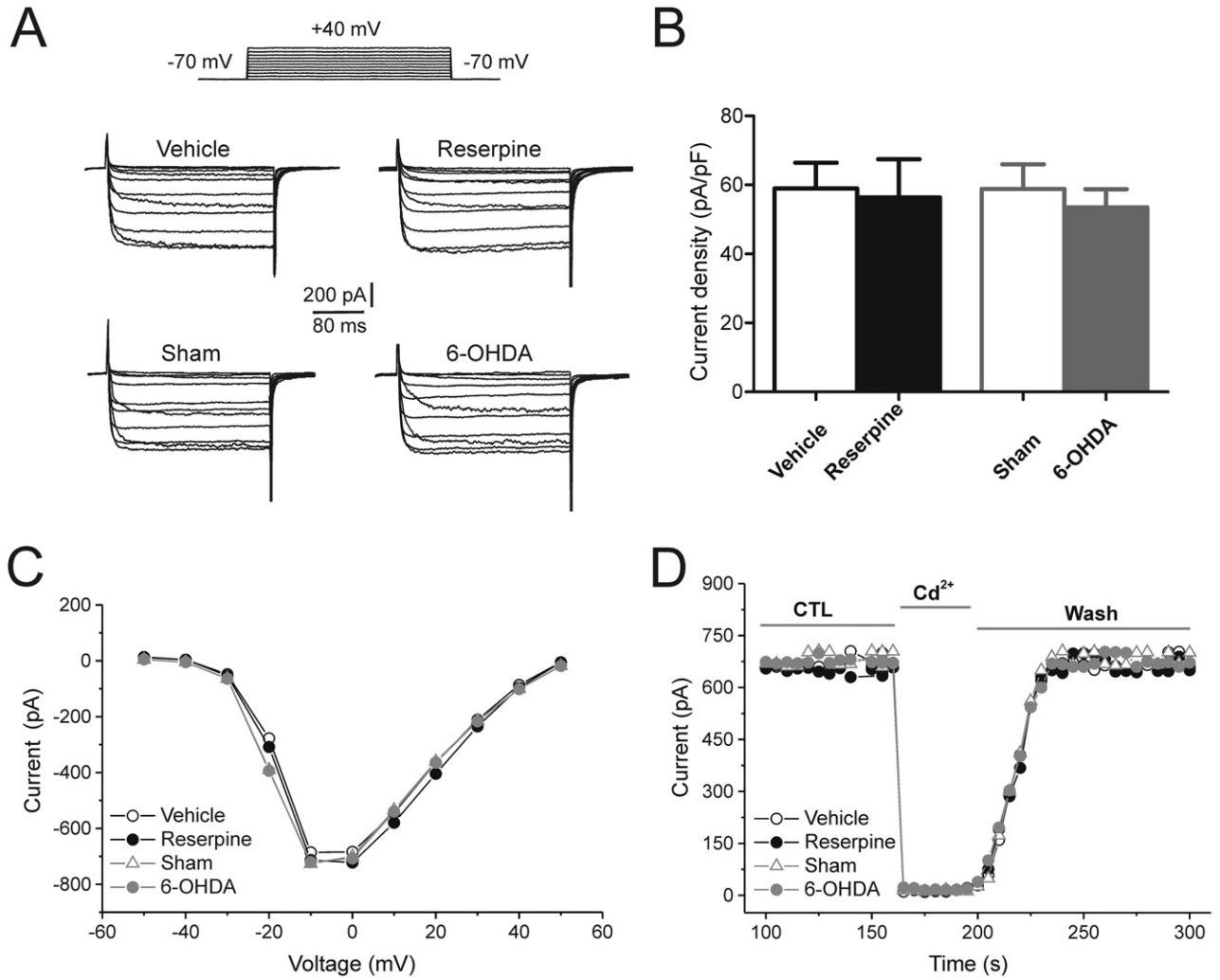

Fig. 1. Analysis of HVA Ca^{2+} currents recorded from MSNs in two different animal models of idiopathic PD. (A) Representative recordings of HVA Ca^{2+} currents from either vehicle- and reserpine-treated rats or 6-OHDA- and sham-lesioned animals. Inward currents were elicited with incremental step commands from −70 to +40 mV. (B) Plot representing the mean±SD of Ca^{2+} current density values (peak current amplitude / whole-cell capacitance). No significant differences were observed in the means among the groups. (C) Representative current–voltage relationship (*I–V* plot) showing HVA Ca^{2+} current half-maximal activation ($V_{½}$), obtained from measurements performed at steady state on the currents shown in (A). (D) Time-course of the effect of cadmium (400 μM) in representative recordings of MSNs from reserpine-treated, 6-OHDA-lesioned, and control rats.

that might affect whole cell current measurement, the whole cell capacitance (CN) was measured for each cell of every experimental group. The mean CN values did not differ among PD models and the respective controls (not shown; vehicle: 10.8±1.3 pF, reserpine: 11.5±2.1 pF, $P>0.05$ Mann–Whitney test; sham: 11.6±1.4 pF, 6-OHDA: 11.6±1.2 pF, $P>0.05$ Mann–Whitney test; $n=10$ for each group; $P>0.05$ ANOVA followed by Tukey HSD test), indicating that the somatic surface area was unchanged. In line with these data, the current/capacitance ratio, that is proportional to current density, did not show significant differences among the experimental groups (Fig. 1B; vehicle: 59.0±7.5 pA/pF, reserpine: 56.4±11.1 pA/pF, $P>0.05$ Mann–Whitney test; sham: 58.8±7.2 pA/pF, 6-OHDA: 53.3±5.3 pA/pF, $P>0.05$ Mann–Whitney test; $n=10$ for each group; $P>0.05$ ANOVA followed by Tukey HSD test).

Similarly, current activation and deactivation kinetics showed no differences among the groups (Fig. 1C; $n=40$ for each group; $P>0.05$ ANOVA, followed by Tukey HSD test). As expected, the recorded Ca^{2+} currents were fully and reversibly blocked by cadmium (Fig. 1D) in all recorded neurons ($n\geq19$, $P<0.05$ Mann–Whitney test).

The contribution of each Ca^{2+} channel subtype to total HVA current was pharmacologically addressed in the two rat PD models and their respective controls by sequentially applying the respective blockers (Fig. 2A). Bath-application of the selective blocker of N-type Ca^{2+} channels, ω-conotoxin GVIA (Ctx-GVIA, 1 μM), produced an inhibitory effect on total HVA current that was not significantly different among the experimental groups (Fig. 2B; $P>0.05$ ANOVA followed by Tukey HSD test). Indeed, 1 μM Ctx-GVIA inhibited Ca^{2+} current by 30.1±6.2% in MSNs from vehicle-treated rats ($n=7$) and by 33.1±5.6% in reserpine-

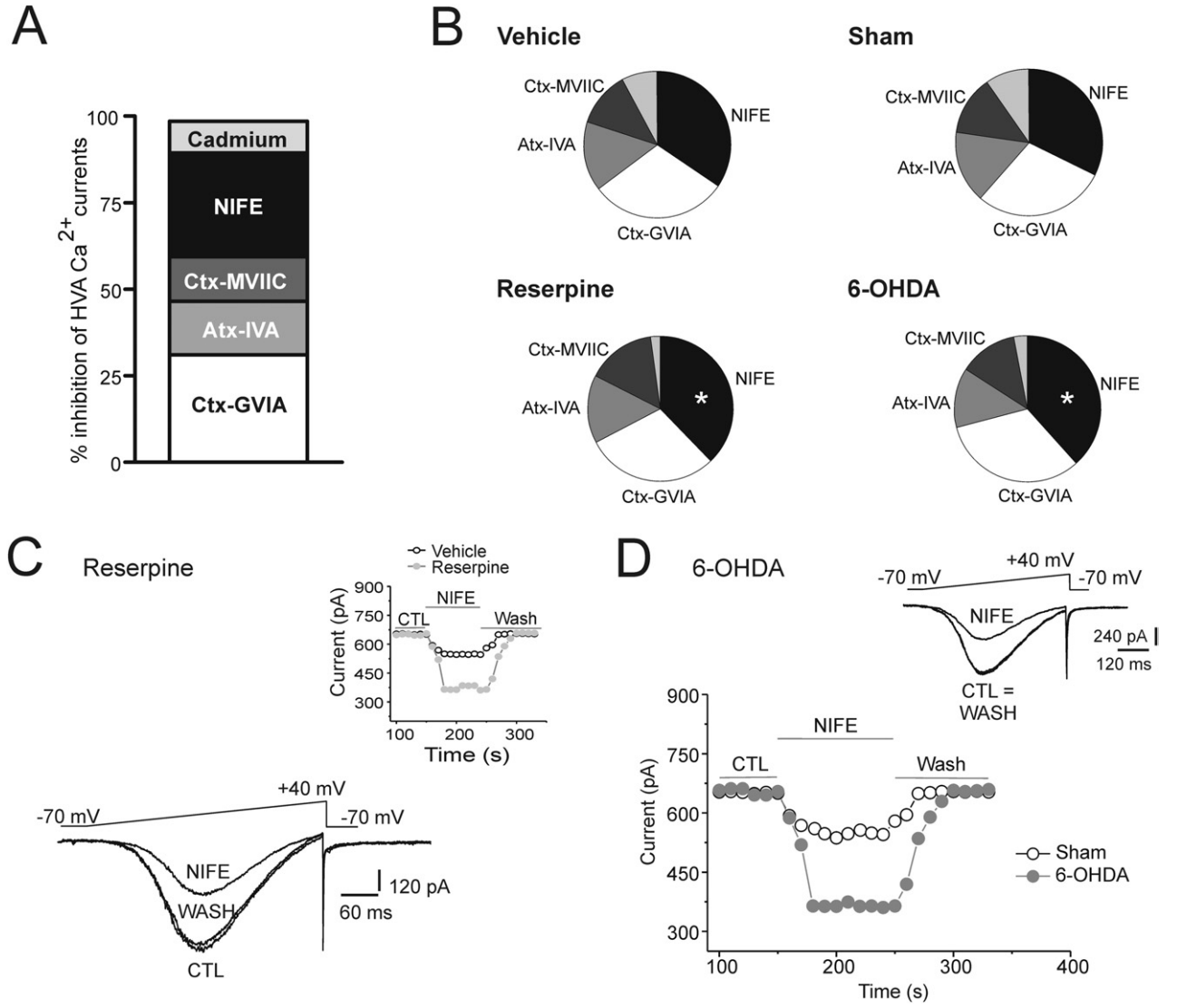

Fig. 2. The dihydropyridine sensitivity of HVA Ca^{2+} currents increases after either reserpine or 6-OHDA treatment. (A) Plot of a representative experiment on a control rat MSN where the single constituents of total HVA Ca^{2+} current were pharmacologically isolated by applying in sequence the selective blockers for L-, N-, Q-, and P-type Ca^{2+} channels (NIFE, Ctx-GVIA, Ctx-MVIIC, and Atx-IVA). Cadmium blocked the residual current. (B) Pie graphs reporting the mean inhibitory values of each channel subtype blocker in the different animal groups. The residual current that was blocked by cadmium is indicated in light grey. *Left*. The NIFE-sensitive component was significantly increased in reserpine-treated rats as compared to vehicle-treated rats. *Right*. A similar increase in the L-type Ca^{2+} current component is observed in 6-OHDA-lesioned rats. Asterisks indicate statistical significance. (C) Representative ramp recording from a reserpine-treated animal. *Inset*: Time-course showing the increased amount of current inhibited by the selective L-type channel blocker NIFE. (D) The time-course plot shows an enhanced NIFE-sensitive component of Ca^{2+} current in a recording from a 6-OHDA-lesioned rat. *Inset*: representative ramp recordings from a 6-OHDA-lesioned rat.

treated animals ($n=7$; Fig. 2B; $P>0.05$ Mann–Whitney test). Similarly, in the sham-operated group Ctx-GVIA caused an inhibition of 28.9±5.3% ($n=8$) vs. 32.1±5.1 in the 6-OHDA-lesioned rats ($n=8$; Fig. 2B; $P>0.05$ *t*-test). The analysis of both P- and Q-type components of HVA Ca^{2+} current in DA depleted animals did not show significant rearrangements in these channels (Fig. 2B). Indeed, the P-type blocker ω-agatoxin IVA (Atx-IVA, 20 nM) caused an inhibition of 15.2±6.7% of total Ca^{2+} current in vehicle-treated rats ($n=5$), vs. 17.0±6.1% in the reserpine-treated group ($n=5$; Fig. 2B; $P>0.05$ Mann–Whitney test). Similarly, no significant difference was observed in the inhibitory effect of Atx-IVA between 6-OHDA- and sham-lesioned rats (16.0±6.1% sham-operated group, $n=8$; 14.2±3.3 6-OHDA-lesioned rats, $n=8$; Fig. 2B; $P>0.05$ *t*-test). Bath-applied ω-conotoxin MVIIC (Ctx-MIIC, 100 nM), selective Q-type channel blocker, reduced total HVA Ca^{2+} current by 12.8±4.5% and 16.8±6.0% in vehicle- and reserpine-treated rats, respectively, and by 13.0±4.1% and 13.4±3.3% in sham- and 6-OHDA-lesioned rats, respectively ($n=5$ for each group; Fig. 2B; $P>0.05$ Mann–Whitney test). Finally, we tested the effect of the dihydropyridine nifedipine (NIFE) at 1 and 5 μM on total HVA Ca^{2+} currents of striatal MSNs. As the results obtained by using

the two doses of NIFE were not statistically different, data were pooled together. Reserpine treatment caused an increase of the inhibitory effect of NIFE to 42.2±5.0% (n=7), with respect to 34.1±6.0% in vehicle-treated rats (n=9; Fig. 2B, C; P<0.001 Mann–Whitney test). A similar increase in the NIFE-sensitive component of total HVA current was observed after 6-OHDA-lesion, as application of the L-type blocker on MSNs from these animals caused an inhibition of 40.4±4.1% in the recorded current, as compared to a reduction of 32.2±5.0% in sham-operated rats (n=6 each group; Fig. 2B, D; P<0.05 t-test).

HVA Ca^{2+} current profile in knockout mouse models of monogenic PD

Next, the channel profile of HVA Ca^{2+} current was analyzed in two knockout mouse models of PD, DJ-$1^{-/-}$ and PINK$1^{-/-}$ mice, and compared to their wild-type littermates (Fig. 3). The amplitude of total Ca^{2+} current recorded from MSNs (Martella et al., 2008) was not statistically different in the four mouse strains analyzed (not shown). Mean HVA Ca^{2+} current amplitude recorded from DJ-$1^{-/-}$ mice was 451.2±30.2 pA (n=16), and 413.9±22.6 pA in their wild-type littermates (n=16; P>0.05 t-test). Similarly, HVA Ca^{2+} current amplitude was 442.8±30.0 pA in MSNs from PINK$1^{-/-}$ mice (n=13) and 452.7±33.2 pA in their wild-type littermates (n=13; P>0.05 Mann–Whitney test).

The CN measurement indicated that the somatic surface area was unchanged among mice groups (P>0.05 ANOVA followed by Tukey HSD test): DJ-$1^{+/+}$ 11.6±1.3 pF, DJ-$1^{-/-}$ 11.7±1.5 pF (not shown; n=10 each; P>0.05 Mann–Whitney test); PINK$1^{+/+}$: 11.5±1.4 pF, PINK$1^{-/-}$ 11.7±0.9 pF (not shown; n=10 each; P>0.05 Mann–Whitney test). Accordingly, the current density, as indicated by the current/capacitance ratio, did not show significant differences among the experimental groups (Fig. 3B; DJ-$1^{+/+}$ 44.5±4.8 pA/pF, DJ-$1^{-/-}$ 49.5±6.1 pA/pF, P>0.05 Mann–Whitney test; PINK$1^{+/+}$ 45.2±6.9 pA/pF, PINK$1^{-/-}$ 43.2±3.7 pA/pF, P>0.05 Mann–Whitney test; n=10 for each group; P>0.05 ANOVA followed by Tukey HSD test). No significant differences in current deactivation or activation were observed among the mice strains, as well (Fig. 3C, D; P>0.05 ANOVA, followed by Tukey HSD test). The recorded currents were fully blocked by 400 μM cadmium (Fig. 3E, F).

The profile of HVA Ca^{2+} current in knockout mouse models of PD was pharmacologically analyzed by applying sequentially the subtype selective channel blockers (Fig. 4). Bath application of 5 μM NIFE reduced the Ca^{2+} current amplitude by 23.0±4.4% in DJ-$1^{+/+}$ mice (n=7), and by 17.1±3.6% in DJ-$1^{-/-}$ mice (n=7; Fig. 4A; P>0.05 Mann–Whitney test). Likewise, NIFE reduced total Ca^{2+} current by a similar extent in PINK$1^{-/-}$ (28.6±5.5%; n=10), and PINK$1^{+/+}$ mice (30.2±6.0%; n=10; Fig. 4C, D; P>0.05 t-test). Interestingly, analysis of N- and P-type HVA Ca^{2+} current fractions gave different results in the two genetic models of PD. In DJ-$1^{-/-}$ mice HVA Ca^{2+} current profiling showed an increased N-type channel-mediated component, with respect to control wild-type littermates (DJ-$1^{-/-}$: 50.0±6.4%; n=5; DJ-$1^{+/+}$: 32.6±5.2%; n=5; Fig. 4A, B; P<0,001 Mann–Whitney test). Conversely, the N-type fraction of Ca^{2+} current was similar in PINK$1^{-/-}$ and PINK$1^{+/+}$ mice (PINK$1^{+/+}$: 24.6±4.1%; n=11; PINK$1^{-/-}$: 20.4±5.0; n=11; Fig. 4C, D; P>0.05 Mann–Whitney). Along with the rearrangement in the contribution of N-type channels to HVA Ca^{2+} current, an increased P-type-mediated component was observed in DJ-$1^{-/-}$ mice. Indeed, Atx-IVA (20 nM) caused an inhibitory effect of 16.3±4.2% in DJ-$1^{+/+}$ (n=5) vs. 30.1±5.7% in DJ-$1^{-/-}$ mice (n=5; Fig. 4A, B; P<0.001 Mann–Whitney test). Again, in PINK$1^{-/-}$ no significant rearrangement of this channel subtype was observed (PINK$1^{+/+}$: 15.2±2.4%; n=6; PINK$1^{-/-}$: 13.4±4.0; n=6; Fig. 4C; P>0.05 t-test). The inhibitory effect of the Q-type Ca^{2+} channel blocker Ctx-MVIIC (100 nM) on total HVA Ca^{2+} current was not significantly altered either in DJ-$1^{-/-}$ or in PINK$1^{-/-}$ mice (DJ-$1^{+/+}$: 19.2±3.1%; n=6; DJ-$1^{-/-}$: 15.7±4.9%; n=7; Fig. 4A; P>0.05 Mann–Whitney test; and PINK$1^{+/+}$: 14.3±3.4%; n=6; PINK$1^{-/-}$: 16.0±4.5%; n=9; Fig. 4C; P>0.05 Mann–Whitney).

Analysis of dopamine-dependent modulation of HVA Ca^{2+} channels in rat and mouse models of PD

Striatal D1 or D2 receptor activation modulates HVA Ca^{2+} channels (Surmeier et al., 1995; Hernandez-Lopez et al., 2000; Pisani et al., 2000). Therefore the altered profile of HVA Ca^{2+} current observed in reserpine-treated and 6-OHDA-lesioned rats, as well as in DJ-$1^{-/-}$ mice, might deeply impact the response to dopamine receptor activation in MSNs. We addressed this issue by analyzing the effect of D1 and D2 receptor activation on HVA Ca^{2+} current in MSNs isolated from animal models of PD. The D1 receptor agonist SKF 83822 (10 μM) caused an inhibition of Ca^{2+} current in most MSNs from control animals (vehicle-treated group: 17.6±4.7%; n=11 out of 13; sham-operated group: 15.6±2.7%; n=11 out of 13; not shown) that was not significantly altered in dopamine-depleted animals (reserpine-treated rats: 15.7±3.2%; n=16 out of 19; 6-OHDA-lesioned rats: 13.1±7.6%; n=13 out of 16; not shown; P>0.05 Mann–Whitney test and ANOVA). Similarly, in both knockout mouse strains, DJ-$1^{-/-}$ and PINK$1^{-/-}$, the effect of D1-like receptor activation was not statistically different from the effect observed in the respective wild-type littermates. Indeed, 10 μM SKF 83822 reduced HVA Ca^{2+} current by 11.7±4.1% (n=8 out of 9) and 13.0±5.5% (n=7 out of 8) in MSNs from DJ-$1^{+/+}$ and DJ-$1^{-/-}$, respectively, and by 16.8±3.9% in 9 out of 11 PINK$1^{+/+}$ cells and 15.3±3.3% in 10 out of 13 PINK$1^{-/-}$ neurons, respectively (not shown; P>0.05 Mann–Whitney test). Bath application of the D1 receptor antagonist SCH23390 (10 μM) prevented the inhibitory effect of SKF 83822 on HVA Ca^{2+} currents in all the animal groups.

Interestingly, we observed a substantial alteration of the quinpirole-mediated modulation of HVA Ca^{2+} currents. Bath application of the D2 receptor agonist quinpirole (10 μM) caused an inhibition of total Ca^{2+} current recorded either from reserpine-treated or 6-OHDA-lesioned rats, that was significantly increased with respect to control

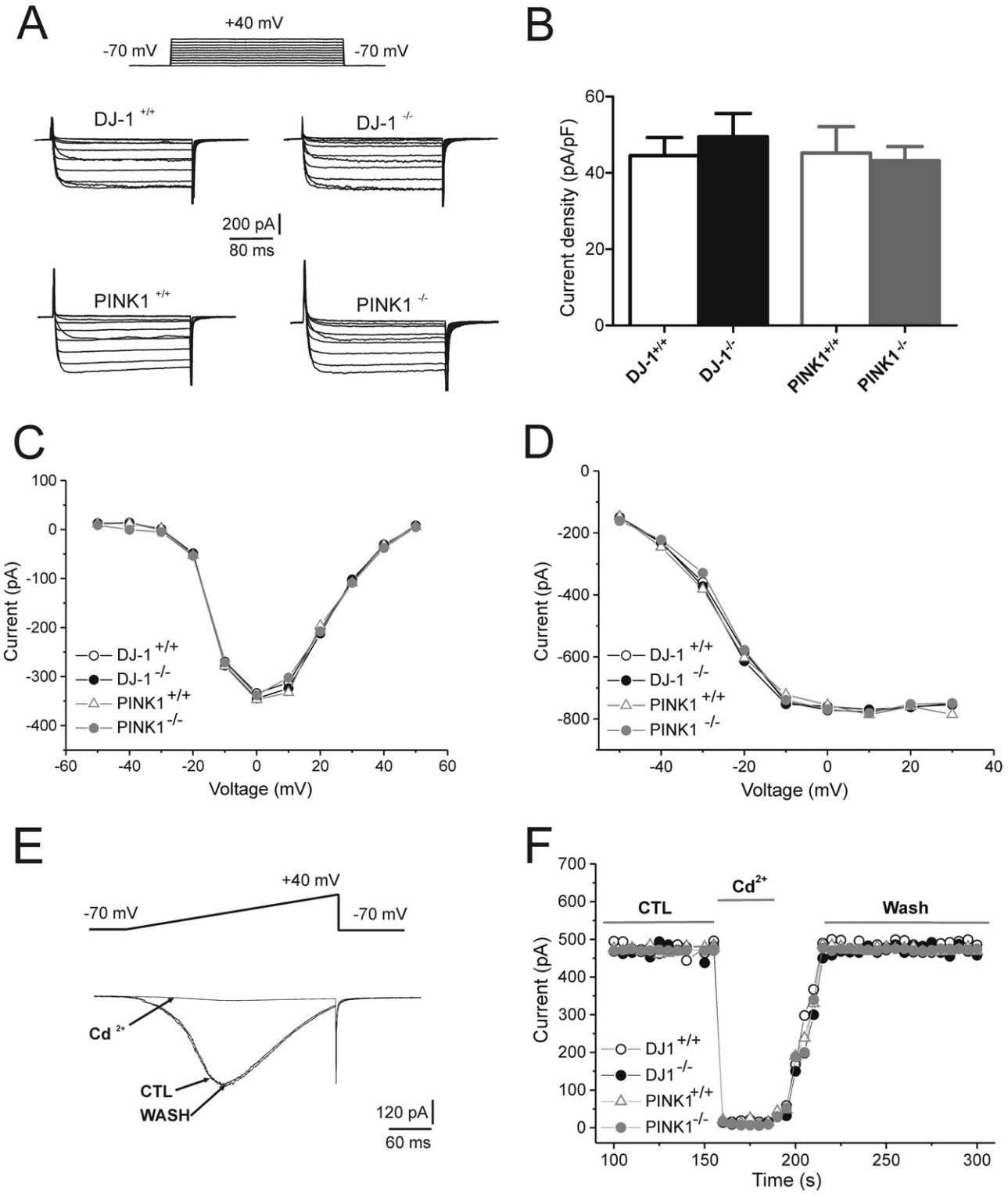

Fig. 3. Analysis of HVA Ca^{2+} currents in two genetic mouse models of PD. (A) Representative recordings showing HVA Ca^{2+} currents evoked from MSNs of DJ1$^{-/-}$ and PINK1$^{-/-}$ mice and their wild-type littermates by means of step commands (from −70 to +40 mV). (B) Plot of HVA Ca^{2+} current density measured from MSNs of the different mouse strains. Data are reported as mean±SD. (C) *I–V* plot of the representative step-evoked Ca^{2+} currents shown in (A). (D) Plot of tail current amplitudes, obtained from the same recordings shown in (A). No significant differences were observed in the properties of HVA Ca^{2+} currents between DJ1$^{-/-}$, PINK1$^{-/-}$ mice, and the respective controls. (E) Representative ramp recording of HVA Ca^{2+} current from a DJ1$^{-/-}$ mouse. Cadmium (400 μM) fully and reversibly blocked the recorded current. (F) Time-course of the effect of cadmium in representative recordings of MSNs from DJ1$^{-/-}$, PINK1$^{-/-}$ mice and the respective controls.

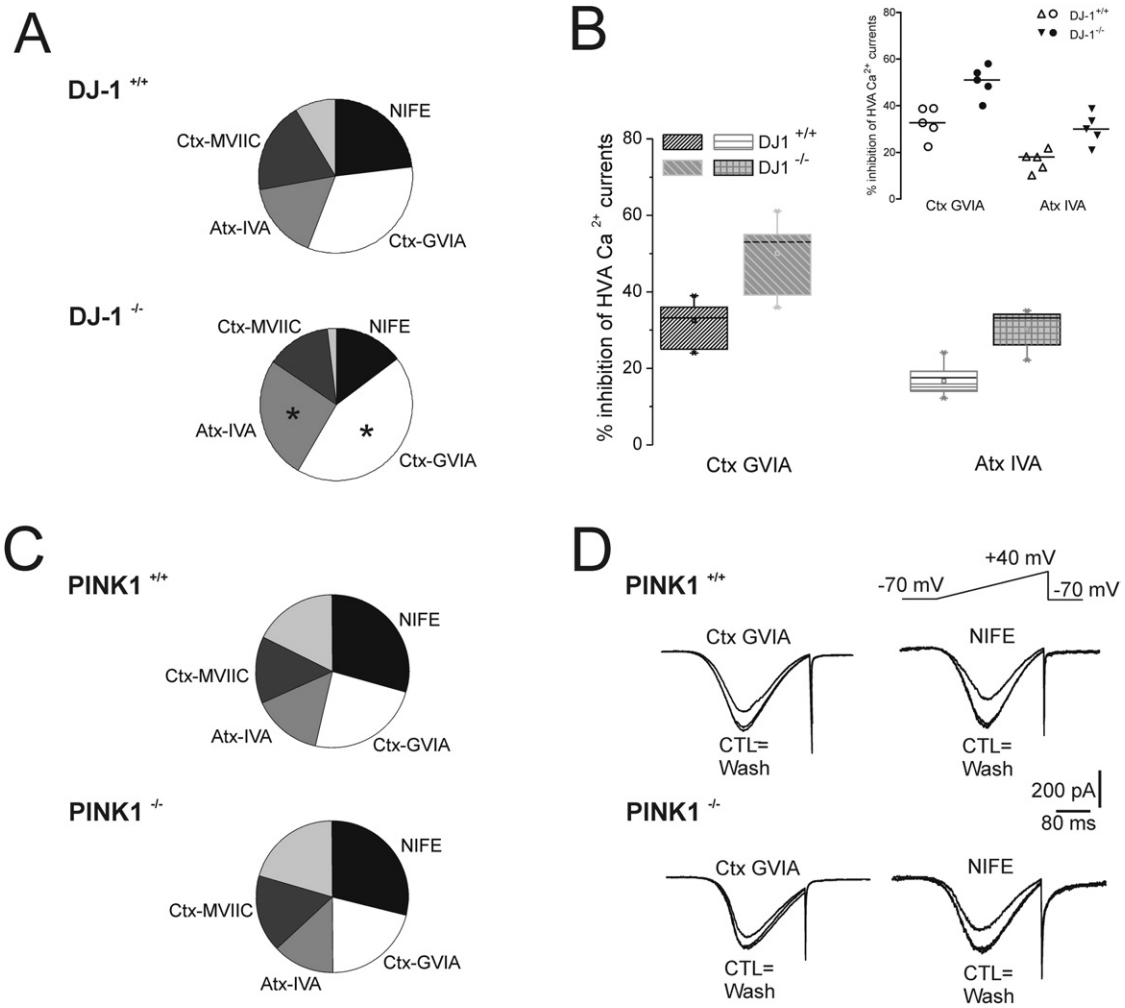

Fig. 4. DJ-$1^{-/-}$ mice show an increase in the Ctx GVIA- and Atx IVA-sensitive components of HVA Ca^{2+} current. (A) Pie plots summarizing the mean portion of HVA Ca^{2+} current inhibited by the selective blockers of L-, N-, Q-, and P-type Ca^{2+} channels, applied in sequence during recordings from DJ-$1^{+/+}$ and DJ-$1^{-/-}$ mice. The residual current that was blocked by cadmium is indicated in light grey. Both the NIFE- and Atx IVA-sensitive components of HVA Ca^{2+} currents were significantly (*) increased in MSNs from DJ-$1^{-/-}$ mice as compared to DJ-$1^{+/+}$ MSNs. (B) Whisker Chart and scatter dot (inset) plots of the inhibitory effect of Ctx-GVIA and Atx-IVA shown in (A). The median value for each experimental group is shown. (C) The mean contribution of each Ca^{2+} channel type to total HVA current is not significantly different in PINK$1^{+/+}$ and PINK$1^{-/-}$ MSNs. (D) Representative recordings of HVA Ca^{2+} current from PINK$1^{+/+}$ and PINK$1^{-/-}$ in the presence of either NIFE or Ctx GVIA, showing no significant difference between the groups.

animals (vehicle-treated: 28.0±4.7%; n=13 out of 15; reserpine-treated: 42.3±7.1%; n=16 out of 19; sham-operated: 27.0±5.4%; n=19 out of 21; 6-OHDA-lesioned: 40.0±7.1%; n=19 out of 23; Fig. 5; $P<0.001$ Mann–Whitney). Similarly, quinpirole caused an increased inhibition of total HVA Ca^{2+} current in MSNs from DJ-$1^{-/-}$ mice (34.7±6.1%; n=5), with respect to the DJ-$1^{+/+}$ group (24.0±7.1%; n=5; Fig. 6A, B; $P<0.001$ Mann–Whitney test). In contrast, we did not observe significant changes in the inhibitory effect of quinpirole on HVA Ca^{2+} current in PINK$1^{-/-}$ mice (24.6±7.1%; n=6 out of 7), compared to PINK$1^{+/+}$ mice (26.4±7.8%; n=6 out of 8; Fig. 6A; $P>0.05$ t-test).

Occlusion experiments with all the selective Ca^{2+} channel blockers were then performed to investigate the channel subtype involved in the altered inhibitory effect of D2 receptor on HVA Ca^{2+} current (not shown). Only NIFE was able to occlude the effect of quinpirole in control rats (vehicle-treated: NIFE 32.1±4.9%; NIFE plus quinpirole 32.1±5.0%; n=5; Fig. 5C; $P>0.05$ Mann–Whitney test; sham-lesioned: NIFE 28.2±3.0%; NIFE plus quinpirole 28.6±4.2%; n=7; Fig. 5C; Mann–Whitney test) and in both groups of DA-depleted animals (reserpine-treated: NIFE 41.2±5.1%; NIFE plus quinpirole 40.0±6.6%; n=7; Fig. 5C; Mann–Whitney test; 6-OHDA-lesioned: NIFE 38.4±4.1%; NIFE plus quinpirole 37.6±5.6%; n=9; Fig. 5C, D; Mann–Whitney test). In PINK$1^{-/-}$ mice, as well as in their wild-type littermates, the quinpirole-mediated inhibitory effect on HVA Ca^{2+} current was fully occluded by the selective N-type channel blocker Ctx-GVIA (PINK$1^{-/-}$ mice: Ctx-GVIA 24.4±4.5%; Ctx-GVIA plus quinpirole 23.9±3.2%; n=6; PINK$1^{+/+}$ mice: Ctx-GVIA 25.2±3.7%; Ctx-GVIA plus quinpirole 24.8±3.3%; n=6; data not shown; $P>0.05$ t-test), while the other Ca^{2+} channel

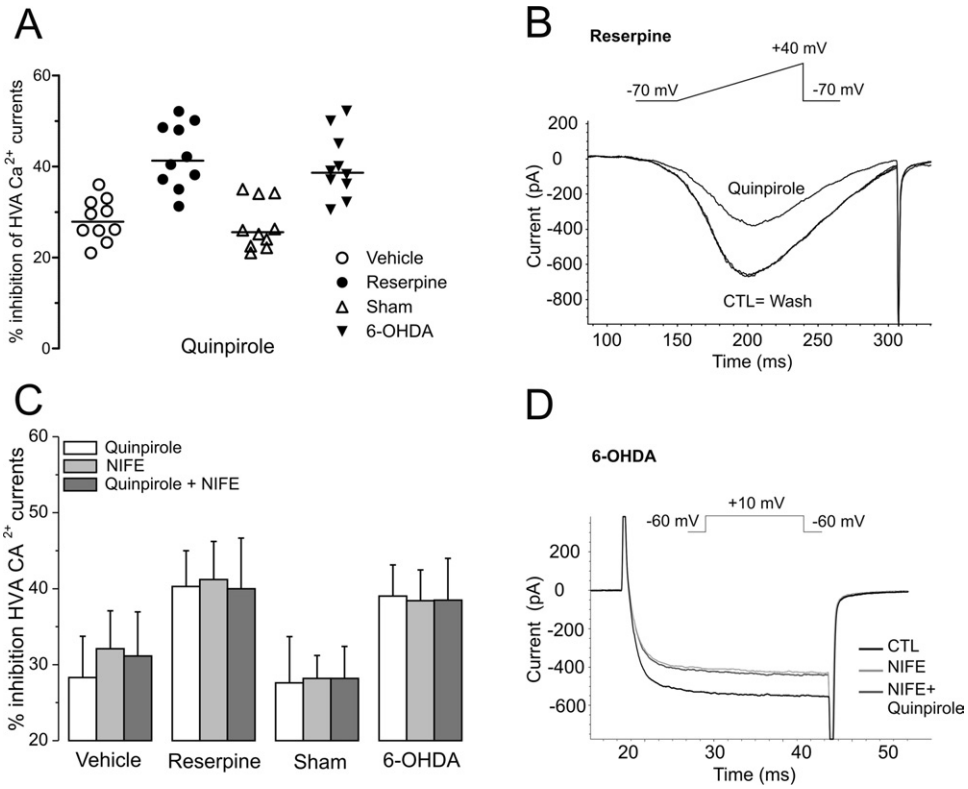

Fig. 5. Increased modulation of L-type channels by D2 receptor in reserpine- and 6-OHDA-treated rats. (A) Scatter dot plot summarizing the inhibitory effect of the D2 receptor agonist quinpirole on reserpine-treated and 6-OHDA-lesioned rats. The graph shows a significantly increased inhibitory effect of quinpirole on both reserpine and 6-OHDA MSNs as compared to the respective controls. To avoid confusion, only 10 values per group have been plotted. The median value for each experimental group is shown. (B) Representative ramp recording (from −70 to 40 mV, 0.3–0.6 mV/ms) of MSN total HVA Ca^{2+} current from a reserpine-treated rat, showing the inhibitory effect of the D2 receptor agonist quinpirole (10 μM). (C) The inhibitory effect of D2 receptor activation is mimicked and occluded by blockade of L-type Ca^{2+} channels in each animal group. (D) Representative recording showing the occlusion by NIFE of the inhibitory effect of quinpirole on step-induced HVA Ca^{2+} current in an MSN from a 6-OHDA-lesioned rat.

blockers tested were ineffective in preventing the inhibitory effect of quinpirole (not shown). Similarly, both in DJ-$1^{-/-}$ and DJ-$1^{+/+}$ mice Ctx-GVIA fully occluded the effect of quinpirole (DJ-$1^{-/-}$ mice: Ctx-GVIA 35.2±4.2; Ctx-GVIA plus quinpirole 35.0±5.9%; n=5; Fig. 6B, C; P>0.05 Mann–Whitney test; DJ-$1^{+/+}$ mice: Ctx-GVIA 26.2±5.9; Ctx-GVIA plus quinpirole 25.0±4.5%; n=6; Fig. 6B; P>0.05 t-test).

DISCUSSION

Acute dopamine depletion induces the upregulation of the D2 receptor-modulated Ca^{2+} currents in rats

The present data show that dopamine depletion following reserpine treatment or 6-OHDA-induced lesion of dopaminergic fibers induces in rat MSNs a rearrangement in the profile of HVA Ca^{2+} channels, with an increase in the L-type component, as well as in their modulation by D2 receptors. While the coupling of D2 receptor to L-type Ca^{2+} channels is not altered by dopamine depletion, the inhibitory effect of its activation on this current component is increased. Indeed, the D2 receptor agonist quinpirole inhibits a larger fraction of total Ca^{2+} current in these animal models than in controls, but its inhibitory effect is occluded by NIFE in both dopamine-depleted rats and controls. This observation is in line with reports suggesting the development of supersensitivity of postsynaptic receptors to dopamine in PD (LaHoste and Marshall, 1993; Bezard and Gross, 1998; Blandini et al., 2000; Zhen et al., 2002; Gubellini et al., 2010). At present it is controversial whether this might be due to an increase in the number of D2 receptors or to an altered D2 receptor-mediated intracellular signaling. Experimental evidence has demonstrated an increased D2 receptor-G_i protein coupling (Rubinstein et al., 1990; Radja et al., 1993; Butkerait et al., 1994; Zhen et al., 2002). The observation that the L-type component of total Ca^{2+} current is increased in MSNs from reserpine and 6-OHDA rats without any change in cell surface area, is in favour of a direct effect of DA depletion on the number/permeability of L-type channels. In fact, overall the present results are consistent with a previous report suggesting the existence of a positive feedback between L-type Ca^{2+} channel activity and the expression of *Cacna1d* gene, coding for the Cav1.3α1 subunit that is selectively targeted by the D2 receptor (Fass et al., 1999; Olson et al., 2005). Acute dopamine depletion following reserpine or 6-OHDA treatment might disinhibit L-type channels and their positive feedback to mRNA expression in MSNs and, in turn, cause the increase in L-type Ca^{2+} current fraction that we observe in our experiments. Most

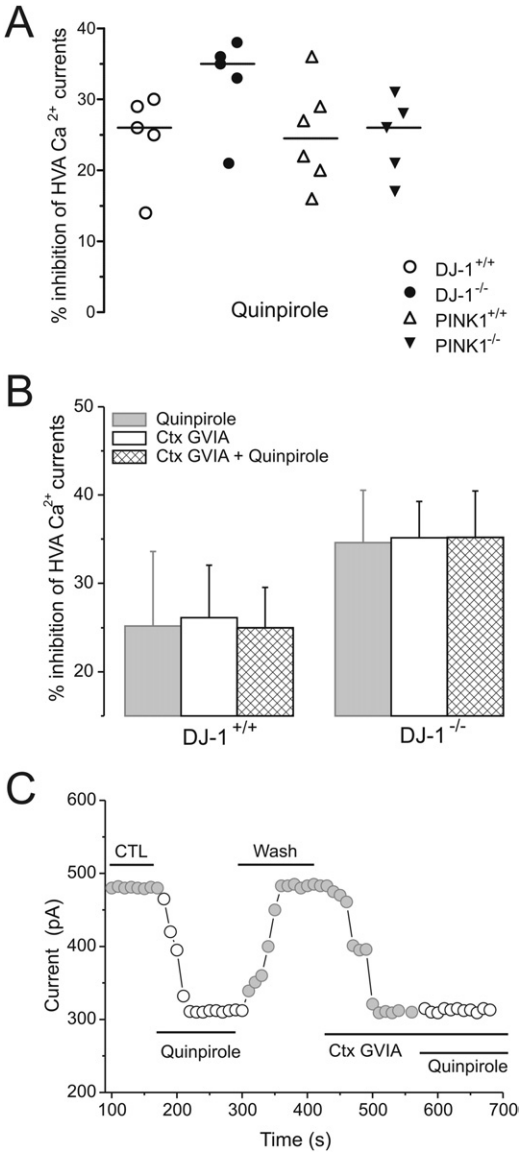

Fig. 6. Increased inhibitory effect of D2 dopamine receptor activation on N-type channels in DJ-1$^{-/-}$ mice. (A) Scatter dot plot of the inhibitory effect of D2 receptor agonist quinpirole on DJ-1$^{-/-}$ and PINK1$^{-/-}$ mice and the respective controls. An increased inhibitory effect of quinpirole on HVA Ca^{2+} current can be observed in MSNs from DJ-1$^{-/-}$ mice, but not in PINK1$^{-/-}$ mice, as compared to the respective wild-type littermates. The median value for each experimental group is shown. (B) Histogram showing that the inhibitory effect of D2 receptor activation is mimicked and occluded by blockade of N-type Ca^{2+} channels in DJ-1$^{-/-}$ mice. (C) Time-course of a representative occlusion experiment in an MSN from DJ-1$^{-/-}$ mice.

recently, Prieto and coworkers (Prieto et al., 2009) performed an analysis of HVA Ca^{2+} current in 6-OHDA lesioned rats. These authors observed a small, non-significant increase in the L-type component recorded from MSNs after 6-OHDA lesion. Though this discrepancy might be due to some methodological differences (6-OHDA dose and age of animals; Salgado et al., 2005; Martella et al., 2008) it is worth noting that we confirmed our findings in a further acute model, reserpine-depleted rats, that is free from adaptive phenomena that might take place after 6-OHDA lesion (Fuentes et al., 2009; Galati et al., 2009).

Striatal MSNs strongly express L-type Ca^{2+} channels containing the Cav1.3α1 subunit at the glutamatergic postsynaptic density in the head of dendritic spines, where they act as negative regulators of spine stability, since deletion of Cav1.3a1 subunits induces spine proliferation and disinhibition induces spine loss (Day et al., 2006). Interestingly, chronic administration of an L-type channel antagonist completely prevented the spine loss induced in MSNs by acute dopamine depletion, suggesting that a reduced dopamine tone might cause the disinhibition of L-type channels, a sustained elevation in intraspine Ca^{2+}, and, in turn, the disassembly of cytoskeleton in spines (Day et al., 2006). Of interest, our data indeed provide direct evidence of an increased L-type component of HVA Ca^{2+} currents, at least at the soma of MSNs from dopamine depleted rats, and further suggest an increased expression of these channels in these models of PD (Fass et al., 1999; Olson et al., 2005).

DJ-1 deletion causes the upregulation of the Ca^{2+} channels modulated by D2 receptor in mice

In MSNs from two genetic mouse models of monogenic PD we observed different profiles of HVA Ca^{2+} currents. Deletion of PINK1 gene did not cause significant rearrangements in Ca^{2+} channels. Conversely, in DJ-1$^{-/-}$ mice we observed an increase in both N- and P-type current fractions. Moreover, in DJ-1$^{-/-}$ mice, similarly to what observed after acute dopamine depletion in rats, D2 receptor activation by quinpirole caused an increased inhibitory effect on Ca^{2+} current.

P/Q-type channels exert a major role in the initiation of action-potential-evoked neurotransmitter release at central nervous system synapses (Pietrobon, 2010), such as striatal GABA release (Arias-Montaño et al., 2007). It is therefore likely, given that the increase in P-type current we recorded at the somatic level was found also at MSNs terminals, that the striatal GABAergic output might be affected in DJ-1$^{-/-}$ mice.

Our data show that the D2 receptor-mediated inhibition of Ca^{2+} current is occluded by Ctx-GVIA in all mice strains, suggesting a preferential action of this receptor on N-type channels in mouse MSNs. A modulatory effect of D2 receptor agonists on N-type channels has been previously described in striatal cholinergic interneurons from both rat and mouse (Yan et al., 1997; Cabrera-Vera et al., 2004; Pisani et al., 2006). Moreover, presynaptic D2 receptors on the terminals of GABAergic afferents to cholinergic interneurons, reported to derive predominantly from striatal MSNs (Bolam et al., 1986; Bennett and Wilson, 1998, 1999), down-regulate GABA release and inhibit $GABA_A$ receptor-mediated postsynaptic potentials by selectively blocking N-type Ca^{2+} channels (Pisani et al., 2000; Momiyama and Koga, 2001). Interestingly, in a heterologous expression system, D2 receptors have been shown to physically interact with N-type channels and regulate their trafficking to the plasma membrane (Kisilevsky and Zamponi, 2008). Indeed, co-expression of the N-type channel

with the D2 receptor produced, in the absence of agonist, a significant increase in channel surface expression. This observation is in line with our data suggesting an increased N-type channel expression in MSNs from DJ-1$^{-/-}$ mice, where a reduced dopamine overflow in the striatum has been reported (Goldberg et al., 2005), and strikingly recalls the modulatory role of D2 receptors on L-type channel expression in MSNs from rats described above, suggesting that this might be a common physiological activity of the D2 receptor displaying specie- and possibly cell-specific features. The apparent discrepancy with other reports showing a modulatory effect of D2 receptors on L-type Ca^{2+} channels in mice (Olson et al., 2005; Day et al., 2006) might be due to a different type of preparation preserving the neuronal processes and/or the age of the animals utilized, as Ca^{2+} currents undergo a profound rearrangement during postnatal development in MSNs (Martella et al., 2008). The observation that the inhibitory effect of D2 receptor activation is occluded by Ctx-GVIA in both DJ-1$^{-/-}$ and wild-type mice demonstrates that the coupling of D2 receptor to N-type Ca^{2+} channels in MSNs from mice is not altered by adaptive mechanisms following DJ-1 deletion, whereas the effect of its activation is increased, thus suggesting the development of supersensitivity of postsynaptic D2 receptors also in this model of monogenic PD, similarly to what is believed to occur in dopamine-depleted animals. Although DJ-1$^{-/-}$ mice have normal numbers of dopaminergic neurons in the SNpc, evoked dopamine overflow in the striatum is markedly reduced, primarily as a result of increased reuptake (Goldberg et al., 2005). It might be speculated that the deletion of PINK1 gene triggers different adaptive mechanisms in MSNs, as in PINK1$^{-/-}$ mice neither the profile of HVA Ca^{2+} channels nor the D2 receptor-mediated modulatory effect are significantly altered. Indeed, though the numbers of dopaminergic neurons and dopamine receptors are unchanged, and evoked dopamine release is reduced similarly to DJ-1$^{-/-}$ mice, however, contrary to DJ-1$^{-/-}$ mice (Goldberg et al., 2005), D2 receptor activation is not sufficient to rescue corticostriatal synaptic plasticity deficits (Kitada et al., 2007). On the other hand, recent experimental evidence has suggested that PINK-1 and DJ-1 might define parallel pathways, partially overlapping downstream, as DJ-1 can partially rescue PINK1 loss in Drosophila (Hao et al., 2010).

CONCLUSION

KO mice are regarded as models of the preclinical changes that might occur due to DJ-1 or PINK1 deficiency in early-onset PD forms (Dawson et al., 2010), while acute dopamine depletion in rats models the more common idiopathic PD. The evidence we reported here of an increased activity of the HVA Ca^{2+} channels selectively modulated by D2 dopamine receptor in MSNs from both dopamine depleted rats and DJ-1$^{-/-}$ mice strongly suggests the convergence of different pathophysiological mechanisms characterized by either acute or inborn striatal dopamine transmission deficits on a common pathway.

These data are in accordance with the hypothesis that striatal dopamine depletion could lead to disinhibition of specific high-voltage-activated calcium channels and, in turn, to striatal spine loss in the parkinsonian condition (Day et al., 2006). Moreover, they might provide a molecular mechanism for the supersensitivity of dopamine D2 receptor reported in animal models and PD patients (La-Hoste and Marshall, 1993; Bezard and Gross, 1998; Blandini et al., 2000; Zhen et al., 2002; Gubellini et al., 2010).

Significant alterations in corticostriatal synaptic plasticity have been described in animal models of acute dopamine depletion (Calabresi et al., 1992, 2007; Pisani et al., 2005; Kreitzer and Malenka, 2007). Also, in DJ-1$^{-/-}$ mice long-term depression (LTD) of corticostriatal synapses is selectively impaired (Goldberg et al., 2005). The expression of LTD requires spine integrity, D1 and D2 receptor activation and a highly regulated Ca^{2+} entry from HVA channels (Calabresi et al., 1992; Bonsi et al., 2003). Therefore, the alteration of the D2-dependent modulation of Ca^{2+} channels observed in both dopamine-depleted and DJ-1 null mice might underlie the absence of LTD.

Accordingly, the hypothesis that Ca^{2+} channel blockers could be effective in the treatment of PD and L-3,4-dihydroxyphenylalanine (L-DOPA)-induced dyskinesias (Rodnitzky, 1999; Chan et al., 2009; Surmeier et al., 2010) is supported by experimental evidence obtained from PD animal models (Day et al., 2006; Meredith et al., 2008; Schuster et al., 2009). Indeed, L-type channel antagonism in 6-OHDA-lesioned rats prevents striatal spine loss and the development of abnormal involuntary movements upon L-DOPA treatment, and attenuates nigrostriatal degeneration in chronic 1-methyl-4-phenyl-1,2,3,6-tetrahydropyridine (MPTP) treated mice.

Acknowledgments—This research was supported by Progetto Finalizzato Regione Sicilia to AP; Progetto Finalizzato Ministero della Salute to PB; NIH R01 NS052745 and R01 NS41779 to JS. The authors wish to thank Mr. Massimo Tolu for excellent technical assistance.

REFERENCES

Arias-Montaño JA, Floran B, Floran L, Aceves J, Young JM (2007) Dopamine d(1) receptor facilitation of depolarization-induced release of gamma-amino-butyric acid in rat striatum is mediated by the cAMP/PKA pathway and involves P/Q-type calcium channels. Synapse 61:310–319.

Baunez C, Nieoullon A, Amalric M (1995) In a rat model of parkinsonism, lesions of the subthalamic nucleus reverse increases of reaction time but induce a dramatic premature responding deficit. J Neurosci 15:6531–6541.

Bennett BD, Wilson CJ (1998) Synaptic regulation of action potential timing in neostriatal cholinergic interneurons. J Neurosci 18: 8539–8549.

Bennett BD, Wilson CJ (1999) Spontaneous activity of neostriatal cholinergic interneurons *in vitro*. J Neurosci 19:5586–5596.

Bezard E, Gross CE (1998) Compensatory mechanisms in experimental and human parkinsonism: towards a dynamic approach. Prog Neurobiol 55:93–116.

Blandini F, Nappi G, Tassorelli C, Martignoni E (2000) Functional changes of the basal ganglia circuitry in Parkinson's disease. Prog Neurobiol 62:63–88.

Bolam JP, Ingham CA, Izzo PN, Levey AI, Rye DB, Smith AD, Wainer BH (1986) Substance P-containing terminals in synaptic contact with cholinergic neurons in the neostriatum and basal forebrain: a double immunocytochemical study in the rat. Brain Res 397: 279–289.

Bonifati V, Rizzu P, Squitieri F, Krieger E, Vanacore N, van Swieten JC, Brice A, van Duijn CM, Oostra B, Meco G, Heutink P (2003) DJ-1(PARK7), a novel gene for autosomal recessive, early onset parkinsonism. Neurol Sci 24:159–160.

Bonsi P, Cuomo D, Martella G, Sciamanna G, Tolu M, Calabresi P, Bernardi G, Pisani A (2006) Mitochondrial toxins in Basal Ganglia disorders: from animal models to therapeutic strategies. Curr Neuropharmacol 4:69–75.

Bonsi P, Pisani A, Bernardi G, Calabresi P (2003) Stimulus frequency, calcium levels and striatal synaptic plasticity. Neuroreport 14: 419–422.

Butkerait P, Wang HY, Friedman E (1994) Increases in guanine nucleotide binding to striatal G proteins is associated with dopamine receptor supersensitivity. J Pharmacol Exp Ther 271:422–428.

Cabrera-Vera TM, Hernandez S, Earls LR, Medkova M, Sundgren-Andersson AK, Surmeier DJ, Hamm HE (2004) RGS9-2 modulates D2 dopamine receptor-mediated Ca2+ channel inhibition in rat striatal cholinergic interneurons. Proc Natl Acad Sci U S A 101:16339–16344.

Calabresi P, Maj R, Pisani A, Mercuri NB, Bernardi G (1992) Long-term synaptic depression in the striatum: physiological and pharmacological characterization. J Neurosci 12:4224–4233.

Calabresi P, Picconi B, Tozzi A, Di Filippo M (2007) Dopamine-mediated regulation of corticostriatal synaptic plasticity. Trends Neurosci 30:211–219.

Chan CS, Gertler TS, Surmeier DJ (2009) Calcium homeostasis, selective vulnerability and Parkinson's disease. Trends Neurosci 32:249–256.

Dawson TM, Ko HS, Dawson VL (2010) Genetic animal models of Parkinson's disease. Neuron 66:646–661.

Day M, Wang Z, Ding J, An X, Ingham CA, Shering AF, Wokosin D, Ilijic E, Sun Z, Sampson AR, Mugnaini E, Deutch AY, Sesack SR, Arbuthnott GW, Surmeier DJ (2006) Selective elimination of glutamatergic synapses on striatopallidal neurons in Parkinson disease models. Nat Neurosci 9:251–259.

Deutch AY, Colbran RJ, Winder DJ (2007) Striatal plasticity and medium spiny neuron dendritic remodeling in Parkinsonism. Parkinsonism Relat Disord 13 (Suppl 3):S251–S258.

Fass DM, Takimoto K, Mains RE, Levitan ES (1999) Tonic dopamine inhibition of L-type Ca2+ channel activity reduces alpha1D Ca2+ channel gene expression. J Neurosci 19:3345–3352.

Fuentes R, Petersson P, Siesser WB, Caron MG, Nicolelis MA (2009) Spinal cord stimulation restores locomotion in animal models of Parkinson's disease. Science 323:1578–1582.

Galati S, Stanzione P, D'Angelo V, Fedele E, Marzetti F, Sancesario G, Procopio T, Stefani A (2009) The pharmacological blockade of medial forebrain bundle induces an acute pathological synchronization of the cortico-subthalamic nucleus-globus pallidus pathway. J Physiol 587:4405–4423.

Goldberg MS, Pisani A, Haburcak M, Vortherms TA, Kitada T, Costa C, Tong Y, Martella G, Tscherter A, Martins A, Bernardi G, Roth BL, Pothos EN, Calabresi P, Shen J (2005) Nigrostriatal dopaminergic deficits and hypokinesia caused by inactivation of the familial Parkinsonism-linked gene DJ-1. Neuron 45:489–496.

Gubellini P, Picconi B, Di Filippo M, Calabresi P (2010) Downstream mechanisms triggered by mitochondrial dysfunction in the basal ganglia: from experimental models to neurodegenerative diseases. Biochim Biophys Acta 1802:151–161.

Hao L-Y, Glasson BI, Bonini NM (2010) DJ-1 is critical for mitochondrial function and rescues PINK1 loss of function. Proc Natl Acad Sci U S A 107:9747–9752.

Harrison MB, Kumar S, Hubbard CA, Trugman JM (2001) Early changes in neuropeptide mRNA expression in the striatum following reserpine treatment. Exp Neurol 167:321–328.

Hernandez-Lopez S, Tkatch T, Perez-Garci E, Galarraga E, Bargas J, Hamm H, Surmeier DJ (2000) D2 dopamine receptors in striatal medium spiny neurons reduce L-type Ca2+ currents and excitability via a novel PLCβ1-IP3-calcineurin-signaling cascade. J Neurosci 20:8987–8995.

Kisilevsky AE, Zamponi GW (2008) D2 dopamine receptors interact directly with N-type calcium channels and regulate channel surface expression levels. Channels (Austin) 2:269–277.

Kitada T, Pisani A, Porter DR, Yamaguchi H, Tscherter A, Martella G, Bonsi P, Zhang C, Pothos EN, Shen J (2007) Impaired dopamine release and synaptic plasticity in the striatum of PINK1-deficient mice. Proc Natl Acad Sci U S A 104:11441–11446.

Kreitzer AC, Malenka RC (2007) Endocannabinoid-mediated rescue of striatal LTD and motor deficits in Parkinson's disease models. Nature 445:643–647.

LaHoste GJ, Marshall JF (1993) New concepts in dopamine receptor plasticity. Ann N Y Acad Sci 702:183–196.

Martella G, Spadoni F, Sciamanna G, Tassone A, Bernardi G, Pisani A, Bonsi P (2008) Age-related functional changes of high-voltage-activated calcium channels in different neuronal subtypes of mouse striatum. Neuroscience 152:469–476.

Meredith GE, Totterdell S, Potashkin JA, Surmeier DJ (2008) Modeling PD pathogenesis in mice: advantages of a chronic MPTP protocol. Parkinsonism Relat Disord 14 (Suppl 2):S112–S115.

Momiyama T, Koga E (2001) Dopamine d(2)-like receptors selectively block N-type Ca(2+) channels to reduce GABA release onto rat striatal cholinergic interneurones. J Physiol 533:479–492.

Olson PA, Tkatch T, Hernandez-Lopez S, Ulrich S, Ilijic E, Mugnaini E, Zhang H, Bezprozvanny I, Surmeier DJ (2005) G-protein-coupled receptor modulation of striatal CaV1.3 L-type Ca2+ channels is dependent on a Shank-binding domain. J Neurosci 25:1050–1062.

Pietrobon D (2010) CaV2.1 channelopathies. Pflugers Arch 460: 375–393.

Pisani A, Bonsi P, Centonze D, Calabresi P, Bernardi G (2000) Activation of D2-like dopamine receptors reduces synaptic inputs to striatal cholinergic interneurons. J Neurosci 20:RC69.

Pisani A, Centonze D, Bernardi G, Calabresi P (2005) Striatal synaptic plasticity: implications for motor learning and Parkinson's disease. Mov Disord 20:395–402.

Pisani A, Martella G, Tscherter A, Bonsi P, Sharma N, Bernardi G, Standaert DG (2006) Altered responses to dopaminergic D2 receptor activation and N-type calcium currents in striatal cholinergic interneurons in a mouse model of DYT1 dystonia. Neurobiol Dis 24:318–325.

Prieto GA, Perez-Burgos A, Fiordelisio T, Salgado H, Galarraga E, Drucker-Colin R, Bargas J (2009) Dopamine d(2)-class receptor supersensitivity as reflected in Ca2+ current modulation in neostriatal neurons. Neuroscience 164:345–350.

Radja F, el Mansari M, Soghomonian JJ, Dewar KM, Ferron A, Reader TA, Descarries L (1993) Changes of D1 and D2 receptors in adult rat neostriatum after neonatal dopamine denervation: quantitative data from ligand binding, *in situ* hybridization and iontophoresis. Neuroscience 57:635–648.

Rodnitzky RL (1999) Can calcium antagonists provide a neuroprotective effect in Parkinson's disease? Drugs 57:845–849.

Rubinstein M, Muschietti JP, Gershanik O, Flawia MM, Stefano FJ (1990) Adaptive mechanisms of striatal D1 and D2 dopamine receptors in response to a prolonged reserpine treatment in mice. J Pharmacol Exp Ther 252:810–816.

Salgado H, Tecuapetla F, Perez-Rosello T, Perez-Burgos A, Perez-Garci E, Galarraga E, Bargas J (2005) A reconfiguration of CaV2 Ca2+ channel current and its dopaminergic D2 modulation in developing neostriatal neurons. J Neurophysiol 94:3771–3787.

Schuster S, Doudnikoff E, Rylander D, Berthet A, Aubert I, Ittrich C, Bloch B, Cenci MA, Surmeier DJ, Hengerer B, Bezard E (2009) Antagonizing L-type Ca2+ channel reduces development of abnormal involuntary movement in the rat model of L-3,4-dihydroxyphenylalanine-induced dyskinesia. Biol Psychiatry 65:518–526.

Smith Y, Villalba R (2008) Striatal and extrastriatal dopamine in the basal ganglia: an overview of its anatomical organization in normal and Parkinsonian brains. Mov Disord 23 (Suppl 3):S534–S547.

Spadoni F, Martella G, Martorana A, Lavaroni F, D'Angelo V, Bernardi G, Stefani A (2004) Opioid-mediated modulation of calcium currents in striatal and pallidal neurons following reserpine treatment: focus on kappa response. Synapse 51:194–205.

Surmeier DJ, Bargas J, Hemmings HC Jr., Nairn AC, Greengard P (1995) Modulation of calcium currents by a D1 dopaminergic protein kinase/phosphatase cascade in rat neostriatal neurons. Neuron 14:385–397.

Surmeier DJ, Guzman JN, Sanchez-Padilla J (2010) Calcium, cellular aging, and selective neuronal vulnerability in Parkinson's disease. Cell Calcium 47:175–182.

Valente EM, Salvi S, Ialongo T, Marongiu R, Elia AE, Caputo V, Romito L, Albanese A, Dallapiccola B, Bentivoglio AR (2004) PINK1 mutations are associated with sporadic early-onset Parkinsonism. Ann Neurol 56:336–341.

Yan Z, Song WJ, Surmeier J (1997) D2 dopamine receptors reduce N-type Ca2+ currents in rat neostriatal cholinergic interneurons through a membrane-delimited, protein-kinase-C-insensitive pathway. J Neurophysiol 77:1003–1015.

Zhen X, Torres C, Cai G, Friedman E (2002) Inhibition of protein tyrosine/mitogen-activated protein kinase phosphatase activity is associated with D2 dopamine receptor supersensitivity in a rat model of Parkinson's disease. Mol Pharmacol 62:1356–1363.

(Accepted 28 December 2010)
(Available online 31 December 2010)